

Enforcing charge conservation in the ALaDyn high-order Pic code

A. SGATTONI¹, P. LONDRILLO², C. BENEDETTI¹, G. TURCHETTI¹
 1-Department of Physics University of Bologna, INFN Bologna
 2-INAf, osservatorio astronomico di Bologna

1. The integration schemes for the Maxwell-Vlasov equations

An improved version of the ALaDyn code is under development and testing. It is designed as a direct extension to higher order of the classical PIC codes, and is then based on the following numerical procedures:

- Time integration for both particles and fields is performed by a three-stage, fourth order Leap-frog scheme.
- Space integration for fields is based on compact, fourth order (C4) or sixth order (C6) schemes applied to field variables (\mathbf{E} , \mathbf{J}) and \mathbf{B} with staggered collocation grid indexing, as in the reference Yee module. Staggering turns out to be a consistent framework for extending charge conservation to higher order schemes.

2. Compact finite differences (CFD) schemes on staggered meshes

Compact high order space derivative provides a powerful technique to achieve spectral-like resolution in wave propagation phenomena. In a uniform grid with spacing h and node points $x_j = jh$, $j = 0, 1, N-1$, we denote grid cells as $C_{j+1/2} = [x_j, x_{j+1}]$ centered at the $x_{j+1/2}$ points. For variables $u_{j+1/2}$ collocated at the cell centers and space derivative u'_j collocated at the cell node points, a compact difference scheme has the form

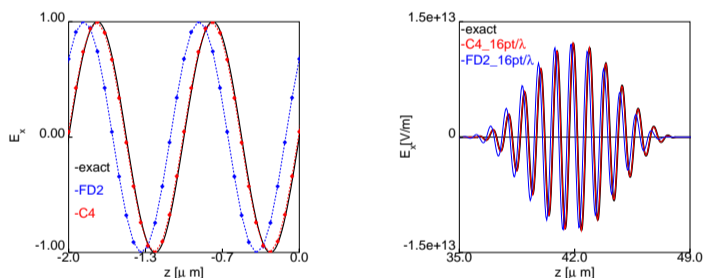
$$u'_j = (\hat{P}^{-1}\hat{Q}[Du])_j, \quad j = 0, 1, \dots, N-1 \quad (1)$$

where \hat{P} and \hat{Q} are band limited, symmetric matrix and $Du = [u_{j+1/2} - u_{j-1/2}]/h$ denotes the standard centered two-point finite difference. In particular, a sixth order compact C6 scheme is obtained with \hat{P} and \hat{Q} both tridiagonal matrix, reducing to fourth order C4 scheme when \hat{Q} is a diagonal matrix.

The classical explicit second order scheme FD2 is recovered when both \hat{P} and \hat{Q} are the identity matrices.

Centered space derivatives of this form have only dispersive numerical errors. For linear problems, the formal accuracy order provides then a direct measure of the accuracy on the wave phase speed.

To illustrate this property, in the following we consider the propagation of a one-dimensional wave packet, modelling a Laser pulse $[E_x(z, t), B_y(z, t)]$ having a \cos^2 envelope shape with $FWHM = 20$ fs and wavelength $\lambda_0 = 0.8\mu\text{m}$.



Left: plane wave propagation for 50 wavelength with 16 points/wavelength
 Right: E_x cut along optical axis of a 2D wave packet evolved for 50 wavelengths
 the shape of the packet changes if propagated using second order of accuracy

3. Extending charge conservation to high order schemes

In a PIC code, charge conservation is designed to assure the discretized continuity equation relating the difference of charge density variable at time levels $t^{(n)}$ and $t^{(n+1)} = t^{(n)} + \Delta t$ to the numerical divergence of the \mathbf{J} current density

$$[\rho^{(n+1)}(\mathbf{x}_g) - \rho^{(n)}(\mathbf{x}_g)] = -\Delta t \hat{\mathbf{D}} \cdot \mathbf{J}^{(n+1/2)}(\mathbf{x}_g) \quad (2)$$

holds at any grid point $\mathbf{x}_g = (x_j, y_k, z_l)$ as an identity. Here the particle density is grid assigned in the usual way, using splines:

$$\rho(\mathbf{x}_g, t) = \frac{1}{\Delta V} \sum_m^{N_m} \hat{S}(\mathbf{x}(t)_m - \mathbf{x}_g) \quad (3)$$

where \hat{S} denotes the tensor product $\hat{S}(\mathbf{x}_m - \mathbf{x}_g) = S(x_m - x_j)S(y_m - y_k)S(z_m - z_l)$ and $\mathbf{x}_m(t)$ denote the particles position. In standard second-order PIC schemes, charge conservation is enforced by defining a current assignment scheme satisfying the continuity condition on each particle, with given positions at time levels n and $n+1$ (Bunemann 1992, Esirkepov, 2001). The discrete continuity equation can be satisfied by solving for the current density directly on the grid defined variables, without any explicit reference to the assignment shape for each particle.

In ALaDyn we implemented this second approach, which is clearly more efficient and can be extended to numerical divergence operators of any kind. In the one dimensional case, if $[D_t \rho]_j = [\rho_j(x^{(n+1)}) - \rho_j(x^{(n)})]$ denotes the charge density difference corresponding to particles positions at different time levels, one solves directly for the grid-defined current density inverting the numerical derivative operator

$$(\hat{P}\hat{Q}[D_x J_x])_j = -\frac{1}{\Delta t} [D_t \rho]_j \quad \text{being } D_x J_x = \frac{1}{\Delta x} (J_{x,j+1/2} - J_{x,j-1/2}) \quad (4)$$

leading to a two-point recursion of a cell averaged density difference:

$$[J_x]_{j+1/2} = [J_x]_{j-1/2} - \frac{D_x}{\Delta t} \hat{Q}^{-1} \hat{P} [D_t \rho]. \quad (5)$$

In the 2D case, the density difference

$$[D_t \rho]_{j,k} = [\rho(x^{(n+1)}, y^{(n+1)}) - \rho(x^{(n)}, y^{(n)})]_{j,k} \quad (6)$$

can be split in a sum of differences along each coordinate component of the particle position using the algebraic identity (Esirkepov)

$$[D_t \rho]_{j,k} = [D_{t,x} \rho]_{j,k} + [D_{t,y} \rho]_{j,k} \quad (7)$$

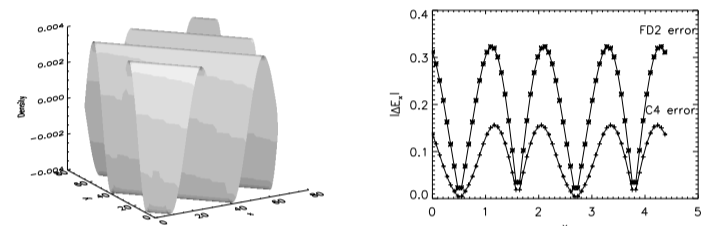
where

$$D_{t,x} \rho = \frac{1}{2} [\rho(x^{(n+1)}, y^{(n)}) - \rho(x^{(n)}, y^{(n)}) + \rho(x^{(n+1)}, y^{(n+1)}) - \rho(x^{(n)}, y^{(n+1)})] \quad (8)$$

$$D_{t,y} \rho = \frac{1}{2} [\rho(x^{(n)}, y^{(n+1)}) - \rho(x^{(n)}, y^{(n)}) + \rho(x^{(n+1)}, y^{(n+1)}) - \rho(x^{(n+1)}, y^{(n)})] \quad (9)$$

The current density components are then defined by solving the one-dimensional recursions for each dimension and the generalization to 3D comes straightforward.

We tested the high-order charge preserving scheme to a pure electrostatic 2D problem, by considering the propagation of linear electron plasma waves across a (x, y) computational plane with periodic boundary conditions.



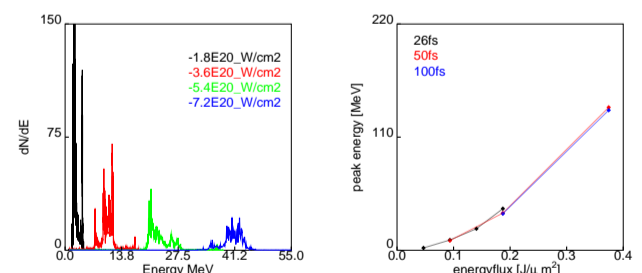
Left: density distribution of a plasma wave propagating with $k_x = k_y$ on the (x, y) computational plane. We used $N_x = N_y = 64$ grid points, 64 particles per cell and 16 grid points per wavelength.
 Right: errors of the computed solutions after $t = 80$ wave periods for a fourth order compact scheme (C4) compared to a classical second order (FD2) scheme.

4. 1-D simulation of ions acceleration

One applications of the modern high power laser pulses is the acceleration of ions: a laser pulse is focalized on a thin solid target, the radiation pressure push forward the electrons creating a big charge separation and a quasi-static electric field that accelerates the ions. The simulation setup of these problem sees a laser pulse focalized on a thin plasma "foil" surrounded by vacuum.

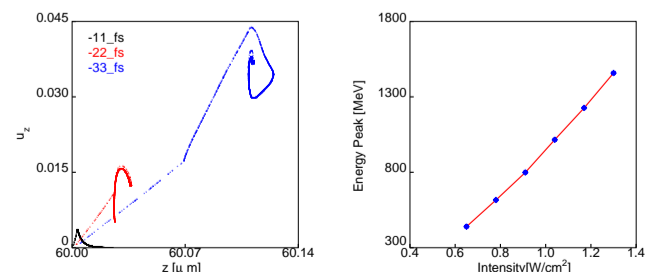
The critical point of a simulation using a PIC code is electron density of the plasma: in an overdense plasma ($n_e > n_c = (\pi m c^2)/(e^2 \lambda_0^2)$) an electromagnetic wave penetrates only on a length of few "skin-depths" $k_p^{-1} = (\lambda_0/2\pi) \sqrt{n_c/n_e}$ and the grid resolution must be high enough to resolve it ($\Delta x < k_p^{-1}$). E.g. : in solid carbon ($n_e \sim 6 \cdot 10^{23} \text{cm}^{-3}$) $k_p^{-1} \sim \lambda_0/150 \Rightarrow$ 3D simulation is beyond nowadays computer performance.

We present some preliminary 1D simulations that show the acceleration dynamics and point out the technique capability. These simulation uses circularly polarized 1D laser pulses following the idea proposed in [T. V. Liseikina, A. Macchi, *Features of ion acceleration by circularly polarized laser pulses*, Applied Physics Letters **91**, 171502 (2007)]



Left: energy spectra of carbon ions from a $0.025\mu\text{m}$ foil $n_e = 4.3 \cdot 10^{23} \text{cm}^{-3}$ illuminated by a laser pulse $FWHM = 26$ fs with different intensities (similar to the laser FLAME of the PLASMON-X experiment)

Right: ions energy peak obtained with the same target, but using different intensities and pulse durations.



Left: ions phase plots for a $FWHM = 26$ fs laser pulse $I = 3.6 \cdot 10^{20} \text{W/cm}^2$ interacting on a $0.025\mu\text{m}$ foil $n_e = 4.3 \cdot 10^{23} \text{cm}^{-3}$

Right: ions energy peak obtained with very high energy pulses with a "flat-top" profile, $FWHM = 100$ fs at different intensities.